Control and Cybernetics

vol. **34** (2005) No. 1

Topology optimization – broadening the areas of application

by

Martin P. Bendsøe[1], Erik Lund[2], Niels Olhoff[2] and Ole Sigmund[3]

[1]Department of Mathematics, Technical University of Denmark
DK-2800 Lyngby, Denmark

[2]Department of Mechanical Engineering, Aalborg University
DK-9220 Aalborg Ø, Denmark

[3]Department of Mechanical Engineering, Technical University of Denmark
DK-2800 Lyngby, Denmark

Abstract: This paper deals with recent developments of topology optimization techniques for application in some new types of design problems. The emphasis is on recent work of the Danish research groups at Aalborg University and at the Technical University of Denmark and focus is on the central role that the choice of objective functions and design parameterization plays for a successful extension of the material distribution approach to new design settings and to new types of physics models. The applications that will be outlined encompass design of laminated composite structures, design for pressure loads, design in fluids, design in acoustics, and design in photonics. A short outline of other design optimization activities is also given.

Keywords: topology optimization, laminates, pressure loads, multiphysics, fluids.

1. Introduction

Topology optimization is now a rather well-established field (for an overview, see, for example, Bendsøe and Sigmund, 2003; Eschenauer and Olhoff, 2001) that after almost two decades of emphasis on structural design is now being applied for optimal design in such diverse areas as electro-magnetism and fluids.

The approach to topology design that we will apply in the following is based on the use of sensitivity analysis and mathematical programming, and the so-called material distribution method is the basis for the design parameterization. The purpose of the design optimization is thus the creation of clear designs that consist of regions within which we have a uniform use of a material, out of

a given set of isotropic or anisotropic materials, including void (for simplicity we denote such designs as black-and-white designs). We do not seek optimal structures that include mixtures of the given materials and thus relaxation and homogenization is not, per se, an integral part of the *design parameterization*.

We note here that other methods for handling the iterative design optimization have been proposed (see Eschenauer and Olhoff, 2001, for an overview). Some of these are based on such concepts as "fully stressed design", while a more recent approach is based on the use of a level-set method, see, e.g., Wang, Wang and Guo (2004) and Allaire, Jouve and Toader (2004), and references therein. In the phraseology of image processing, the material distribution method and the level-set approach are both concerned with segmentation and one can see many analogies between the basic concepts of image segmentation and the field of topology design (this is for example clearly illustrated in Bourdin and Chambolle, 2003).

In the material distribution method for topology design one typically works with a fixed finite element grid model of a structural domain and introduces a parameterization of material through one or more material densities, together with constitutive models that relate these densities to physical parameters. This can be stiffness for structures, but the concept can just as well be applied in other physics models and can describe such diverse material properties as thermal conduction, magnetic permeability, porosity, etc. In this way the concept from structural stiffness design can be transformed to a broader range of applications and this is the theme for this paper.

The extension of the methodology is, notwithstanding the uncomplicated statement above, not trivial. A typical question is how to make a physically realistic relation between density and physical properties that also allows for the goal of obtaining black-and-white designs. An equally important issue is how to formulate objective functions and constraints so that the design optimization results are useful from an engineering point of view. For both issues it is also important to bear in mind that the resulting problems should be computationally tractable.

2. The basics of the material distribution method

In order to set the scene for the developments of the paper, we will here consider the problem of topology design for maximum stiffness of statically loaded linearly elastic structures. This problem is equivalent to design for minimum compliance c defined as the work done by the loading against the displacements at equilibrium.

The FEM format of the minimum compliance problem for a structure with given loading and prescribed volume V is shown below. For computations we apply a mathematical programming algorithm and use the standard nested format for formulating design optimization problems. Thus, we write the problem

as a problem in the design variables only:

$$\begin{aligned} &\min_{\boldsymbol{\rho}} \; c(\boldsymbol{\rho}) \\ &\text{s.t.} : \sum_{e=1}^{N} v_e \rho_e \leq V, \quad 0 < \rho_{\min} \leq \rho_e \leq 1, \quad e = 1, \ldots, N \; . \end{aligned} \tag{1}$$

The equilibrium equation is considered as part of a function-call that gives the value of the objective function $c(\boldsymbol{\rho})$ (assuming linear behaviour):

$$c(\boldsymbol{\rho}) = \mathbf{f}^T \mathbf{u} \; , \quad \text{where } \mathbf{u} \text{ solves} : \quad \mathbf{K}(\boldsymbol{\rho})\mathbf{u} = \mathbf{f} \; , \tag{2}$$

where $\mathbf{u}$ and $\mathbf{f}$ are the displacement and load vectors, respectively. The stiffness matrix $\mathbf{K}$ depends on the vector $\boldsymbol{\rho}$ of the element-wise constant *materal densities* in the elements, numbered as $e = 1, \ldots, N$, in such a way that we can write $\mathbf{K}$ in the form

$$\mathbf{K}(\boldsymbol{\rho}) = \sum_{e=1}^{N} \rho_e^p \; \mathbf{K}_e \; , \tag{3}$$

where $\mathbf{K}_e$ is the (global level) element stiffness matrix for element e.

For the mathematical programming approach, gradients are typically required by the optimization algorithm employed to solve (1) and these can be derived directly or by use of the well-known *adjoint* method.

In the formulation above, we work on a *fixed* FEM mesh that describes the design domain (the reference domain) and the structure is defined as a raster image by the densities ρ_e. Also, the load $\mathbf{f}$ is in this basic formulation design independent and is given in relation to the fixed mesh.

An important issue in the model problem shown here is the relation between density and stiffness. In (3) we have used the so-called SIMP-model that models stiffness as proportional to density in the power p where $p > 1$. In this way intermediate densities are penalized (the volume is linear in $\boldsymbol{\rho}$) and if one uses $p \geq 3$ the result of the optimization is typically black-and-white (Bendsøe and Sigmund, 2003).

The apparent simplicity of the problem statement above belies the fact that several issues have to be handled in an implementation. Firstly, the problem size means that FEM calculations and choice of optimization algorithm are important; this is today mostly an issue in 3D calculations. Secondly, the problem statement should be augmented by some scheme that will make the results mesh-independent and which removes checkerboards that can appear in the computations. There are various ways to do this, with the application of some type of filtering technique becoming the most popular concept; such techniques typically also assure existence of solutions in a continuum format of the problem. These aspects are discussed in more detail in Bendsøe and Sigmund (2003) where also relevant references can be found. For the simple

minimum compliance problem shown here a complete program for 2D problems including filtering, FEM analysis, optimization (by a simple optimality criterion algorithm), and display of results can be written in 99 lines of Matlab code (Sigmund, 2001).

2.1. Extensions

The problem statement above has been the starting point for the development of methods for topology design in a broad range of structural design settings as well as in other areas of engineering, and a few of the more recent developments are illustrated below. In these new problems one keeps the basic format of the design parameterization, the problem statement, and the computational procedure. However, several issues need to be addressed. These encompass the formulation of objective functions and constraints that results in useful engineering designs. Also, a central issue is how to relate grey-scale (density) to physical properties that allow for an evaluation of these objective functions and constraints. Finally, some scheme should be imposed to obtain black-and-white designs. These issues should all be handled in such a way that checkerboards and mesh-dependency are avoided (see Sigmund and Petersson, 1998 and also Bendsøe and Sigmund, 2003, for an overview) and (preferably) such that some form of existence result can be obtained for the continuum setting of the problem.

3. New structural mechanics applications

3.1. Design with pressure loads

In the prototype problem (1) the load has to be defined in relation to the *fixed* FEM mesh of the reference domain. For *pressure loads* we have a situation where the external loads depend on the boundary between solid and void and because of the design parameterization as a grey-scale raster representation one does not have boundaries that are well defined. This means that topology design with pressure loads is a highly challenging problem that does not directly fit into our generic framework.

The differences in the definitions and results of the prototype problem (1) for optimal design with fixed surface loading and a corresponding problem of topology optimization with hydrostatic surface pressure loading are illustrated in Figs. 1 (b) and 1 (c) by the solutions obtained to two such problems. Note that the pressure loading in Fig. 1 (c) is design-dependent, i.e., both the locations and directions of the loading change with change of the design.

Topology design with surface pressure loading was first undertaken by Hammer and Olhoff (2000, 2001), Chen and Kikuchi (2001), Bourdin and Chambolle (2003), and Du and Olhoff (2004a) for 2D problems with static loading (a related problem for distributed surface loads was treated in Fuchs and Moses, 2000). A method for 3D problems is published by Du and Olhoff (2004b), and

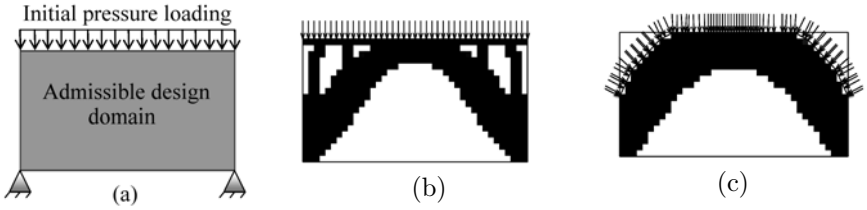

Figure 1. Difference in topology design results. (a) Admissible design domain (volume fraction of material 50%), boundary conditions, and initial loading conditions. Optimal topologies for the problems of optimizing with (b) fixed surface loading, and (c) hydrostatic surface pressure loading.

an extension to topology design with time-harmonically varying hydrodynamic pressure loading is presented in Olhoff and Du (2004).

The compliance of the structure subject to static pressure loads is written as

$$c(u) = \int_{\Omega} bu \, \mathrm{d}\Omega + \int_{\Gamma_t} tu \, \mathrm{d}\Gamma + \int_{\Gamma_p} pu \, \mathrm{d}\Gamma, \tag{4}$$

where an extra term representing the design dependent load – here a pressure p – acting on parts of the boundary Γ_p of the *material domain* (b is a body force and t a boundary traction at a fixed boundary).

In the work of Hammer and Olhoff (1999, 2000) and the extensions by Du and Olhoff (2004 a, b), the optimization process is performed by successive iterations making use of the finite element analysis model with fixed mesh on the one hand, and the design model with the parameterized iso-volumetric density surface for the pressure loading on the other. The load surfaces in the design model are controlled by the density distribution in the finite element model and in turn fully determine the global load vector on the finite element model. Thus, the sensitivity analysis is based on both the analysis model and the design model. In the sensitivity analysis also the sensitivities of the load vector with respect to a design change must be evaluated, and this is done analytically. The problem is solved by an optimality criteria method.

3.1.1. Design with hydrodynamic pressure loads

In the design of structures and machines against vibration and noise, many problems are concerned with hydrodynamic surface pressure loading that varies harmonically in time. For such problems it may be an important design objective to determine the structural topology that minimizes the dynamic compliance associated with a prescribed exitation frequency and amplitude of the hydrodynamic surface pressure loading (Olhoff and Du, 2004).

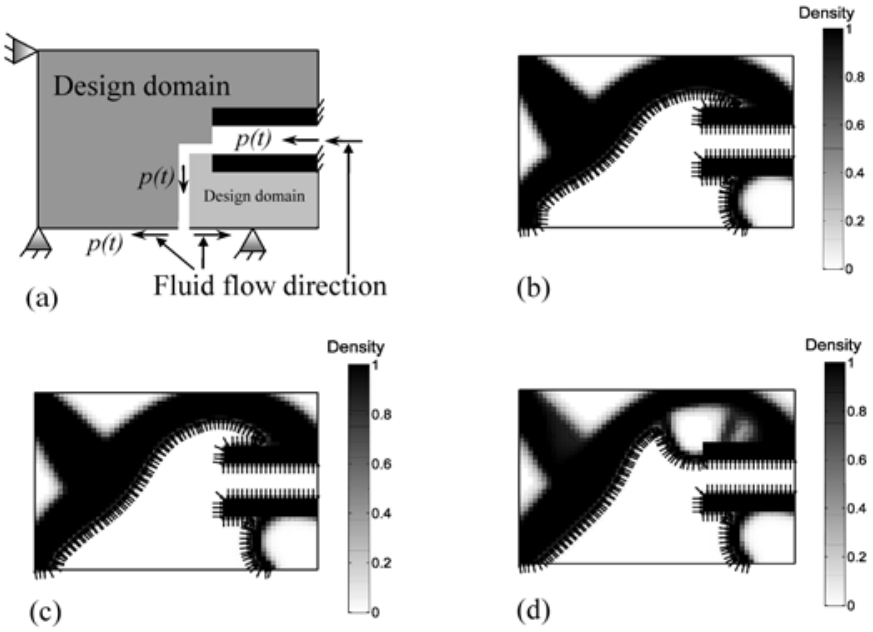

Figure 2. Topology optimization of an inlet and pressure chamber subjected to time-harmonic hydrodynamic pressure loading, with minimization of the dynamic compliance as the design objective. The optimization is performed for three different prescribed frequencies ω of the loading. (a) Admissible design domain (with 40% volume fraction of material) and boundary conditions. Optimal topology designs obtained for the given loading frequencies (b) $\omega = 0$ (static loading), (c) $\omega = 800$ and (d) $\omega = 1000$.

This problem constitutes an extension to the prototype topology design problem (1) and the design problem with hydrostatic pressure loads considered above. Relative to equations (1)–(3), the mathematical formulation of the problem consists of (1) with $c(\boldsymbol{\rho})$ replaced by a new objective function $c_d(\boldsymbol{\rho})$ defined by the equation

$$c_d(\boldsymbol{\rho}) = \mathbf{f}^T \mathbf{u} \,, \quad \text{where } \mathbf{u} \text{ solves :} \quad \big(\mathbf{K}(\boldsymbol{\rho}) - \omega^2 \mathbf{M}(\boldsymbol{\rho})\big)\, \mathbf{u} = \mathbf{f}(\boldsymbol{\rho}) \,. \tag{5}$$

In (5), ω denotes the given circular exitation frequency and $\mathbf{f}$ is the global vector of amplitudes of the design-dependent hydrodynamic pressure loads, while $\mathbf{M}$ and $\mathbf{u}$ denote the global mass matrix and displacement amplitude response vector, respectively.

The example in Fig. 2 models the inlet from a channel to a larger pressure chamber subjected to a fluid with a time-harmonically varying hydrodynamic

pressure. The material around the inlet is prescribed to be solid and non-changeable. Here, two domains of the structural surface are acted upon by the fluid as shown along with the admissible design domain in Fig. 2 (a). The design objective is minimization of the dynamic compliance (which is equivalent to maximization of the integral dynamic stiffness of the structure). The figure shows the optimized topologies for the three prescribed loading frequencies $\omega = 0$ (static loading) in Fig. 2 (b), $\omega = 800$ in Fig. 2 (c), and $\omega = 1000$ in Fig. 2(d). It is seen that when the loading frequency is increased from 0 to 800, the optimal topology of the structure remains the same while the shape is slightly changed. When the loading frequency is increased to 1000, both the topology and the shape of the structure are changed.

3.2. Laminated composite structures

The use of fiber reinforced polymers (FRP) in structural design has gained an ever increasing popularity due to their superior mechanical properties and this section focuses on the use of ideas from multi-material topology optimization for optimal design of composite laminate shell structures, especially wind turbine blades. These structures consist of stiff fiber reinforced polymers or soft core materials stacked in a number of layers and bonded together by a resin, and the design problem is to determine the stacking sequence by proper choice of material and fiber orientation of each FRP layer in order to obtain the desired structural performance. For complicated geometries like wind turbine blades this is a very challenging design problem that calls for use of sophisticated structural optimization tools.

Different approaches for changing the parameterization of the problem have been investigated. In Foldager, Hansen and Olhoff (1998, 2001), ply angles were used as design variables and the problem of non-convexity was avoided by using the well-established technique of converting the lay-up expressed in terms of ply angles and ply thicknesses to an expression in terms of lamination parameters (see Hammer, Bendsøe, Lipton and Pedersen, 1997, and references therein). In each step of the optimization process identification methods were used in Foldager et al. (1998) for converting the optimized pseudo layup described by lamination parameters to a physical layup described by ply thicknesses and angles. This method is applicable to all types of laminates and loading cases, since the feasible domains for the lamination parameters are not needed in the process.

Another parameterization approach is called the Discrete Material Optimization (DMO) method, see Lund and Stegman (2005) and Stegman and Lund (2005), and it is based on the mixed materials strategy suggested by Sigmund and co-workers (Sigmund and Torquato, 1997, Gibiansky and Sigmund, 2000) for multi-material topology optimization, where the total material stiffness is computed as a weighted sum of candidate materials.

In the present context this means that the stiffness of each layer of the lam-

inated composite structure will be computed from a weighted sum of a finite number of "plausible" constitutive matrices, each representing a given lay-up of the layer. Consequently, the design variables are no longer the fiber angles or layer thicknesses but the scaling factors (or weight functions) on each constitutive matrix in the weighted sum. For example, we could choose a stiff orthotropic material oriented at three angles $\theta_1 = 0°$, $\theta_2 = 45°$ and $\theta_3 = 90°$ and a soft isotropic material, thereby obtaining a problem having four design variables per layer. The objective of the optimization is then to drive the influence of all but one of these constitutive matrices to zero for each ply by driving all but one weight function to zero. As such, the methodology is very similar to that used in topology optimization. This is further emphasized by the fact that penalization is used on the design variables to make intermediate values un-economical. At the beginning of the optimization, the constitutive matrices used in the analysis thus consist of contributions from several candidate materials, but at the end of the design optimization, the parameterization for the weight functions has to fulfill the demand, that one distinct candidate material has been chosen.

3.2.1. Parameterization

As in topology optimization the parameterization of the DMO formulation is invoked at the finite element level. The element constitutive matrix, $\mathbf{C}^e$, for a single layered laminate structure may in general be expressed as a sum over the element number of plausible material configurations, n^e:

$$\mathbf{C}^e = \sum_{i=1}^{n^e} w_i \mathbf{C}_i \tag{6}$$

where each "plausible" material is characterized by a constitutive matrix $\mathbf{C}_i$. The interpolation of true material density is done in a similar way. The weight functions w_i must all have values between 0 and 1 in order to be physically allowable. Furthermore, in case of solving eigenfrequency problems or having a mass constraint, it is necessary that the sum of the weight functions be 1.0, i.e., $\sum_{i=1}^{n^e} w_i = 1.0$.

Several new parameterization schemes have been developed, and we give here a short outline of the most effective implementation (for other possibilities, see Stegman and Lund, 2005). We apply for each element a number of design variables ρ_i^e, $i = 1, \ldots, n^e$, and write

$$\begin{aligned} w_i^e &= \frac{\hat{w}_i^e}{\sum_{k=1}^{n^e} \hat{w}_k^e}, \quad i = 1, \ldots, n^e \\ \hat{w}_i^e &= (\rho_i^e)^p \prod_{j=1;\ j\neq i}^{n^e} \left(1 - (\rho_j^e)^p\right) \ . \end{aligned} \tag{7}$$

To push the design variables ρ_i^e towards 0 and 1 the SIMP method has been adopted by introducing the power, p, as a penalization of intermediate values of ρ_i^e. Moreover, the terms $(1-\rho_j^e)_{j\neq i}$ are introduced such that an increase in ρ_i^e results in a decrease of all other weight functions. Finally, the weights have been normalized in order to satisfy the constraint that the sum of the weight functions is 1.0. Note that the expression (7) means that complicated additional constraints on the design variables ρ_i^e are avoided and only simple box constraints have to be dealt with.

In order to further reduce the existence of intermediate values of the weight functions at the end of the optimization process, an explicit penalization method has been implemented. This method is applied when, for example, 50 design iterations have been performed and it computes a penalization term that is added to the objective function. The penalization term W_{penal} is computed as

$$W_{\text{penal}} = S_{\text{fac}} \sum_{i=1}^{I} w_i^q (1 - w_i^q) \tag{8}$$

where q is a power, typically 2, and the penalization scale factor S_{fac} is set such that the contribution from W_{penal} on the sensitivities is of the same order of magnitude as the original sensitivities of the objective function. In this way all weight functions, w_i, are forced to 0 or 1 which is useful when the parameterization given by (7) is used. However, the explicit penalization requires some tuning of S_{fac} to perform well and thus is problem dependent.

The only difference between single and multi layered laminate structures is that the interpolation given above has to be used for all layers, i.e., the layer constitutive matrix $\mathbf{C}^l$ is computed as

$$\mathbf{C}^l = \sum_{i=1}^{n^l} w_i \mathbf{C}_i \tag{9}$$

where l denotes "layer" and thus n^l is the number of plausible materials for the layer.

The design variables ρ_i may be associated with each finite element of the model or the number of design variables may be reduced by introducing patches, covering larger areas of the structure. This is a valid approach for practical design problems since laminates are typically made using fiber mats covering larger areas.

3.2.2. Optimization of wind turbine blade main spar

In order to demonstrate the potential of the method, maximum stiffness design of a generic main spar model provided by the wind turbine manufacturer Vestas Wind Systems A/S is studied. A slightly different version of this example is published in Lund and Stegmann (2005). It should be noted that this is a

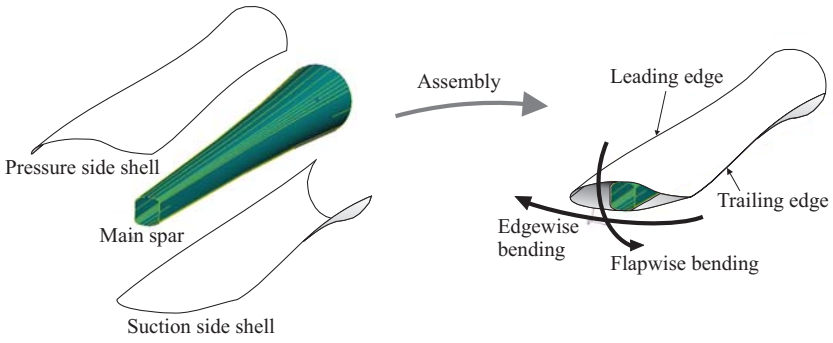

Figure 3. Load carrying main spar from a wind turbine blade. Courtesy of Lennart Kühlmeier, Vestas Wind Systems A/S.

preliminary study, and thus, the main goal with the example is to demonstrate the method on a complicated design problem.

The wind turbine blade basically consists of two structural components, the main spar and the aerodynamic shell, see Fig. 3.

The main spar carries most of the flapwise bending loads whereas the shell carries most of the edgewise bending loads. In this study the main spar is subjected to the most critical load case which is the flapwise bending load that arises when the turbine has been brought to a standstill due to high wind and the blade is hit by the 50 year extreme wind.

In the model used only the main spar is considered, i.e., the two shell parts are removed. In order to account for their contribution to the stiffness of the main spar, the thicknesses of the shells in direct contact with the main spar are added to the top of the flanges of the main spar. Thus, the local stiffness contribution is included but the support conditions from the shells are ignored. The finite element model used is shown in Fig. 4 and consists of 9600 four node shell elements.

The finite element model of the main spar is divided into 77 patches, i.e., regions with the same layup and thickness. The length of the part of the main spar studied is 15 meters and the flapwise bending is applied using two nodal forces at the end as shown in Fig. 4. The model is clamped at the root end, i.e. all displacements and rotations are fixed. With these boundary conditions the dominant state will be bending, which results in tension/compression in the top and bottom flanges and shear in the wedges. Furthermore, due to the geometry of the spar, which twists its cross section along the length due to aerodynamic considerations, the spar will also be subjected to torsion when subjected to flapwise bending. These basic considerations will be used as a guideline for interpreting the results of the optimization.

For the stiffness optimization problem it has been chosen first to use patch

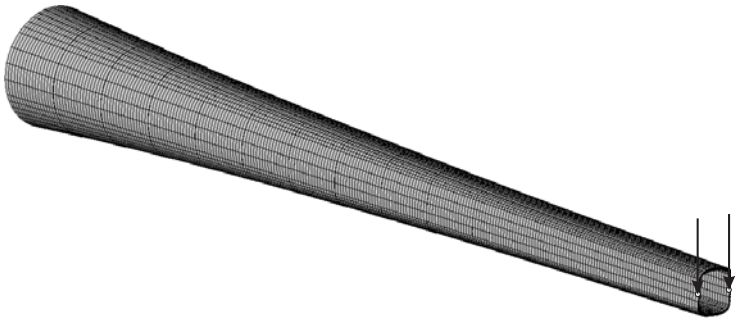

Figure 4. Finite element model with loads used for maximum stiffness design of the load carrying main spar.

design variables, i.e, the design variables will be linked to all finite elements associated with a given patch covering a larger area of the main spar, and next the design variables are associated to each finite element.

There are two materials, a stiff GFRP material and a softer isotropic material, and the mass constraint is set such that 15% of the total volume should be filled with soft material. The number of layers for the patch design variable model is set to 16, and the soft material can only be chosen for the 14 interior layers since this material is not a realistic choice for the skin layers. For simplicity, the GFRP material can only be oriented at $0°$, $\pm 45°$, and $90°$, and therefore the number of design variables is 4 for the inner and outer layers, and 5 for all 14 interior layers. The total number of design variables becomes 6006. All layers in a given patch have uniform thicknesses, and the overall thickness is equal to the original one in each patch.

In Fig. 5 the optimized material directions for the glass fiber are shown for the 16 layers. If the soft material has been chosen, then no directions are shown. Layer 1 is the inner (bottom) layer and layer 16 the outer (top) layer.

The results for the patch design variable model suggest that several layers are quite similar, and therefore 8 layers have been chosen for the element-wise design variable model in order to reduce the number of design variables. Again, only stiff material can be chosen in the skin layers, and the number of design variables for this model becomes 364800. The results for the element-wise design variable model can be seen in Fig. 6.

The two optimization models yield quite similar results and, as expected, most of the soft material has been put in the webs in the internal layers close to the root of the main spar in lightly stressed areas. Looking at the two models in detail it is apparent that the element-wise design variable model shown in Fig. 6 chooses to use soft material in all internal layers of the web, distributed continuously over approximately the first third of the main spar. In contrast the

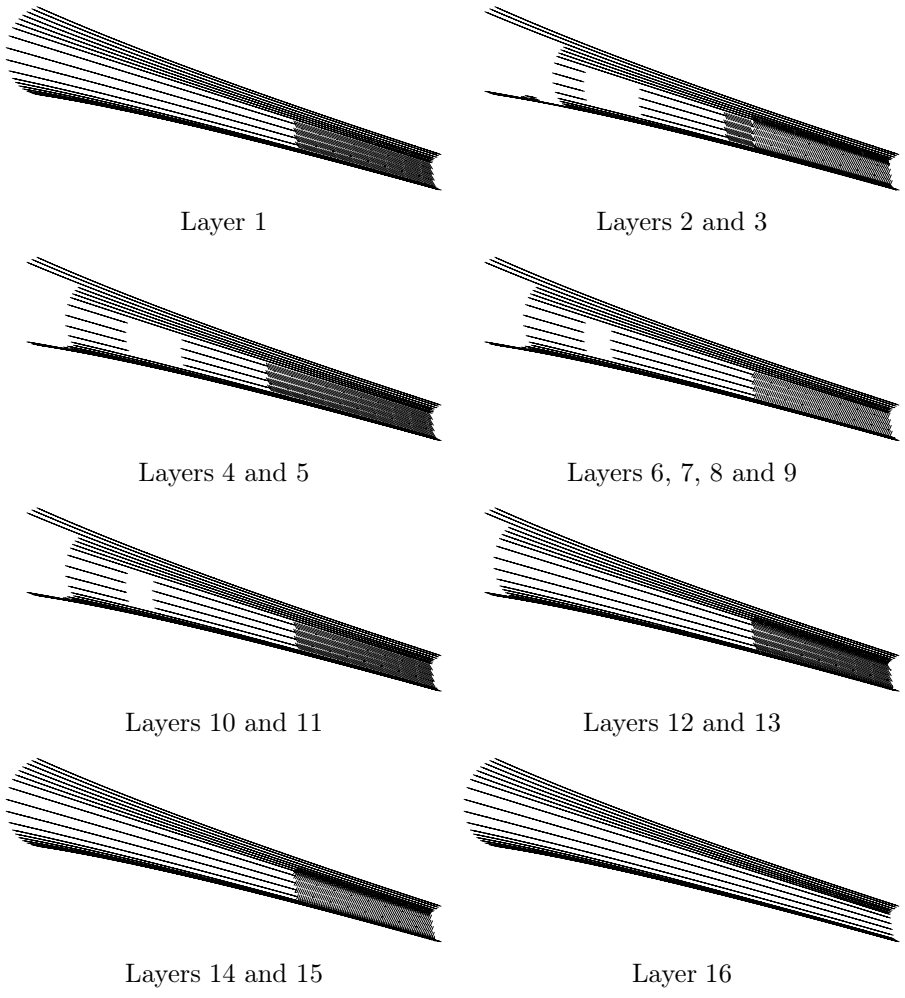

Figure 5. Optimized material directions for the GFRP material in the 16 layers using 77 patches. There are 4 DMO variables (0°, ±45°, and 90°) for the GFRP material, and void indicates that the soft material has been chosen.

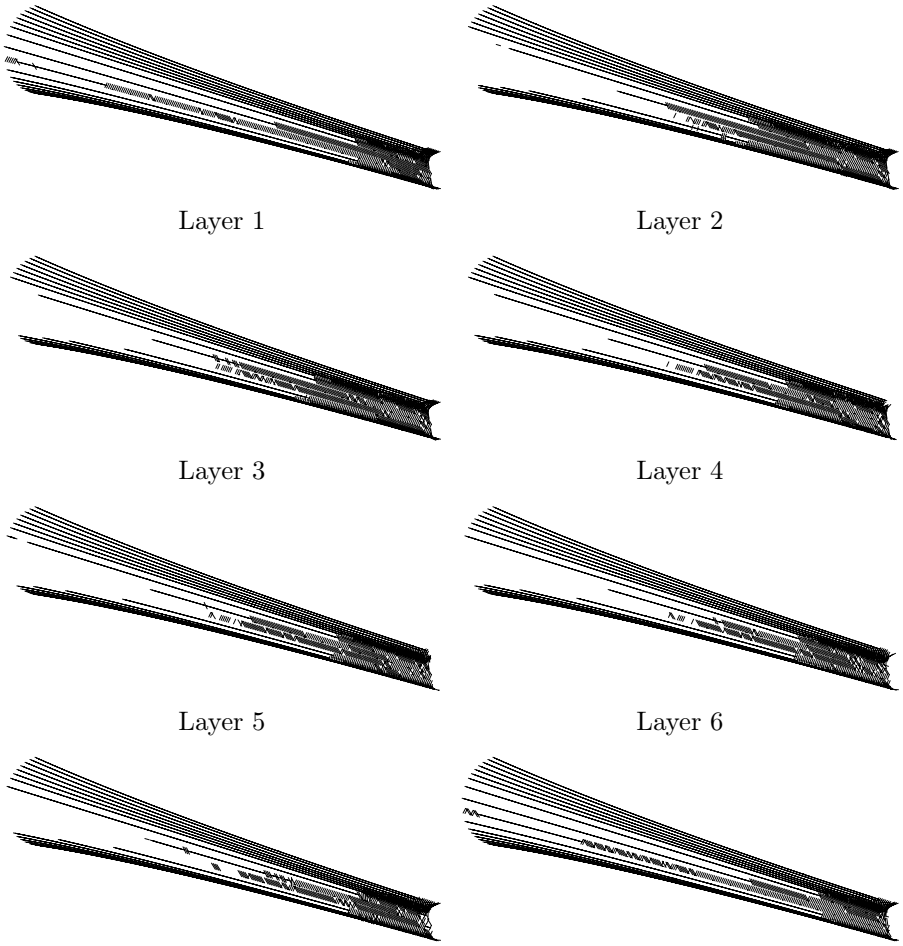

Figure 6. Optimized material directions for the GFRP material in all 8 layers using element-wise design variables. There are 4 DMO variables (0°, ±45°, and 90°) for the GFRP material, and void means that the soft material has been chosen.

patch design variable model in Fig. 5 only places soft material in parts of the internal layers in two distinct regions rather than continuously. This illustrates that choice of material and orientation for each patch is a compromise between all elements in the patch while in the element-wise design variable model, the properties of each element can be set individually.

The orientation of the GFRP material also corresponds well to what was expected from the basic considerations made earlier regarding the load carrying mechanisms of the spar. In the flanges all layers are dominated by 0° orientation, i.e. along the length of the spar, to account for bending while the webs are dominated by $\pm 45^\circ$ to account for shear in the element-wise design variable model. Due to the compromises made over larger areas in the patch design variable model most of the GFRP material in the webs is oriented at 0° because the bending load dominates the patches in the webs. In both models most GFRP material in the last third of the webs is oriented at $\pm 45^\circ$ due to shear and some torsion as the main spar is slightly twisted along the length.

The patch design variable solution is by far the easiest to realize, from a manufacturing point of view, since it encompasses large and well defined regions as opposed to the complex solution of the element-wise design variable model. However, the results will depend on the chosen patches and as such the element-wise design variable model gives much more detail about the best solution.

The results presented here are somewhat crude in that only five candidate materials have been used, and the natural next step would be to expand the design space and allow for a larger variation of fiber angles in order to obtain a more detailed design. However, Figs. 5 and 6 still illustrate very well the potential of the method to solve the combinatorial problem of proper choice of material, stacking sequence and fiber orientation simultaneously on a real life complicated structure like a wind turbine blade main spar for maximum stiffness design.

4. Other physics models

Recently, the topology optimization method has been extended and applied in several other physics settings than that of structures. We will here briefly discuss two of these applications namely the application in wave-propagation problems and the application in fluid problems.

4.1. Wave propagation problems

The governing equation for a number of different wave-propagation problems is the scalar Helmholtz equation

$$\nabla \cdot (A \nabla u) + \omega^2 B u = 0, \tag{10}$$

where, depending on the physics problem considered, the field u (in 2D or 3D) as well as the material constants will have different physical meanings. For the

case of acoustic waves, u is the pressure, A is the inverse of the mass density and B is the inverse of the bulk modulus. For the case of elastic shear waves, u is out of plane elastic displacements, A is the shear modulus and B is the mass density. For the case of planar transverse electromagnetic polarized waves (the TE-mode), u is the electric field, A is the inverse of the dielectric constant and B is the product of the vacuum permitivity and vacuum permeability, whereas for the other polarization (transverse magnetic waves - the TM-mode), u denotes the magnetic field value, $A = 1$ and B equals the product of the dielectric material value, the vacuum permitivity and the vacuum permeability. Hence, if one can perform topology optimization in problems modelled by the Helmholtz equation, simple exchange of parameter values allows one to perform optimization of several different physics problems.

Different goals for the optimization may be considered and after some experimenting it has been found useful to apply either the so-called Poynting vector in order maximize the wave energy transport or to extremize a local amplitude measure. The latter measure is defined as

$$\hat{u}_{\text{out}} = \frac{1}{\Omega_{\text{out}}} \int_{\Omega_{\text{out}}} |u| \; d\Omega, \tag{11}$$

i.e., the average of the magnitude of the field in the output region Ω_{out} which is a subset of the total design domain Ω. The Poynting vector (see, e.g., Landau and Lifshitz, 1975) averaged over a time-period is for this scalar case calculated as

$$\mathbf{I} = \frac{\omega}{2} \int_{\Gamma_{\text{out}}} A\Re(i \; u \; \nabla \overline{u}) \; d\Gamma, \tag{12}$$

where Γ_{out} is a line through which the energy flow is measured and $\Re$ denotes the real part of a complex number.

Boundary conditions for the governing equation (11) may be of Neumann, Dirichlet or absorbing type and we also use Perfectly Matching Layers (PML) to exclude any unwanted boundary effects from absorbing boundaries.

The topology optimization problem in discretized form may now be written as

$$\begin{aligned} \min_{\boldsymbol{\rho}} \quad & c = \Phi(\mathbf{u}) \\ \text{s.t.:} \quad & (\mathbf{K} + i \; \omega \; \mathbf{C} - \omega^2 \mathbf{M}) \; \mathbf{u} = \mathbf{f} \; , \\ & \sum_{e=1}^{N} v_e \rho_e \leq V, \qquad 0 < \rho_e \leq 1, \quad e = 1, \ldots, N \; , \end{aligned} \tag{13}$$

where $\mathbf{K}$, $\mathbf{C}$ and $\mathbf{M}$, are the stiffness, damping and mass like system matrices resulting from the discretization of the Helmholtz equation (11) and the boundary conditions. For this problem the sensitivities of the objective function can be obtained by the adjoint method.

The material properties in these design problems are for simplicity (see comments below) interpolated *linearly* between the two material phases, i.e.

$$\begin{aligned} A(\rho_e) &= \rho_e A_1 + (1-\rho_e)A_2 \\ B(\rho_e) &= \rho_e B_1 + (1-\rho_e)B_2. \end{aligned} \tag{14}$$

In many applications discrete solutions with distinct material phases (no intermediate values of ρ) are automatically the outcome of the optimization process since maximum contrast gives the best wave-confinement. However, in some cases "grey solutions" with intermediate densities may appear. In those cases $0-1$ designs can be obtained by introducing some artificial damping in one of the material phases or we introduce a penalization damping term (we call it the "pamping" term) which introduces artificial high damping in intermediate density elements. This procedure is described in detail elsewhere (Jensen and Sigmund, 2005).

Otherwise, the implementation follows the standard density based topology optimization approach as described in detail by Bendsøe and Sigmund (2003) and the optimization method is the Method of Moving Asymptotes, see Svanberg (1987, 2002).

4.1.1. Example: Acoustics

We show one example of topology optimization of wave propagation problems applied to the design of an inverse acoustic horn. The design problem is sketched in Fig. 7a. The square shaped modelling domain (filled with air) has absorbing boundary conditions and there is an incoming wave over the mid-half of the left boundary. At the right boundary there is a channel through which we want to maximize the energy flow by distributing 25% aluminum in the design domain (dotted rectangle). The objective function is thus defined as the maximization of the horizontal component of the Poynting vector (12) in the channel.

The correct physical modelling of this problem would require a complicated model with coupling between the acoustic waves in air and elastic waves in the aluminum. However, due to the huge impedance ratio between air and aluminum, waves propagating through air will hardly enter into the aluminum and therefore we can model the hole problem by the Helmholtz equation. This assumption has been verified by numerical tests. A thin wall of aluminum in the modelling domain efficiently stops wave propagation. The material properties we use are $\rho_{\text{air}} = 1.3kg/m^3$, $\rho_{\text{alu}} = 2643kg/m^3$, $\kappa_{\text{air}} = 141kN/m^2$ and $\kappa_{\text{alu}} = 68.7GN/m^2$.

We perform the topology optimization for three different wave loads. First we optimized the material distribution for loading frequency $\omega = 0.07$. The resulting horn is shown in Fig. 7b and the frequency response is shown in the bottom of Fig. 7. Then we optimized the material distribution for loading frequency $\omega = 0.15$. The resulting horn is shown in Fig. 7c. We note that the higher the

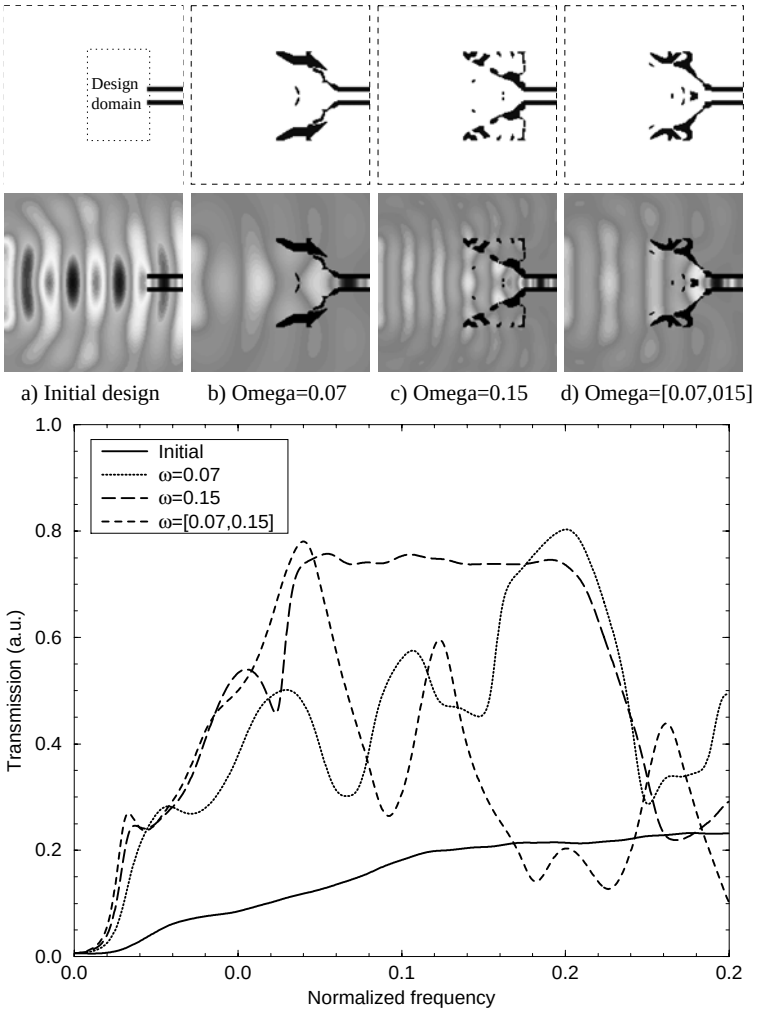

Figure 7. Topology optimization of a wave propagation problem. Top: a) initial design and wave pattern, b) topology optimized inverse horn for $\omega = 0.07$, c) topology optimized inverse horn for $\omega = 0.15$ and d) topology optimized inverse horn for the frequency interval $\omega = [0.07, 0.15]$. Bottom: Frequency response for the 4 structures.

frequency, the more fragmented and irregular the optimized structure becomes. This can be understood by considering that the wavelength becomes smaller for the higher frequency and since the wave shape determines the topology, the resulting topology is likely to have finer details for higher frequencies[1].

From the frequency response plot (bottom of Fig. 7) we see that both designs have high transmission values for the frequencies they are optimized for but they have fairly bad transmission for other frequencies. In order to obtain a structure that is good for a wider frequency band, we solve a max-min problem consisting in maximizing the minimum of 10 transmission values in the frequency interval $\omega = [0.07, 0.15]$. Since the minimum values may change during optimization, we developed an active set strategy, where the frequencies of the minimum transmission values in 10 sub-intervals are updated every 10 iterations based on a Padé approximation of the frequency response (see Jensen and Sigmund, 2005, for more details). The resulting structure is seen in Fig. 7d and we note that the frequency response is now almost constant and high over the considered interval although not as efficient as the one-frequency-optimized structures at their optimization frequencies.

Many more examples of topology optimization in wave-propagation problems are given in the references Borel et al. (2004), Jensen (2003), Sigmund and Jensen (2003, 2005), and Jensen and Sigmund (2004, 2005).

4.1.2. Example: A Z-bend in photonics

The planar photonic crystal is an optical nano-material with periodic modulation of the refractive index. The modulation is designed to forbid propagation of light in certain wavelength ranges, so-called photonic bandgaps. Breaking the crystal symmetry by introducing line defects and other discontinuities allows for control of the light on a sub-wavelength scale in the photonic crystals. Therefore, photonic devices based on the bandgap effect may be up to one million times smaller than traditional integrated optical devices.

The idea behind these devises are as follows. Light propagates as waves and if transmitted through a transparent medium like glass, it will propagate essentially without losses. However, if one perforates the glass structures with a periodic arrangement of air holes with hole distances a little less than the wave length of the light (this means that we are talking about length scales smaller than micrometers, i.e. nano-scale), waves at certain frequencies will no more propagate through the glass structure. This effect can be used to produce mirrors in nano-scale or it can be used to guide light in optical chips. The latter can be obtained by filling some of the air holes in channel-like patterns as seen for a Z-bend in Fig. 8. Since the light cannot travel through the perforated structure, it will stay within the channel and can be led around sharp corners

[1] Another effect of the wave-dependency of the optimized topologies is that we rarely see mesh-depedency. This may be explained by the wave length imposing a length scale in the design problem.

and may be manipulated in other ways. Such photonic crystal structures will in the future provide the basic building blocks for optical devices and computers.

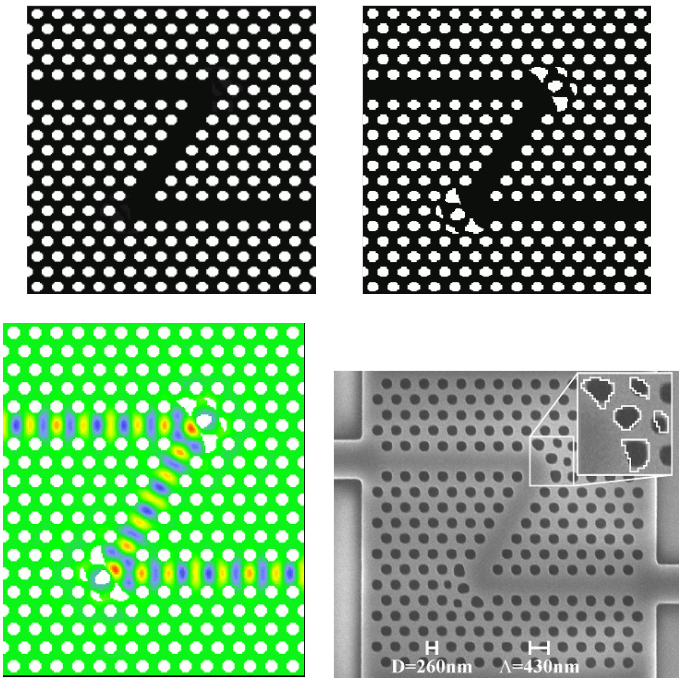

Figure 8. Top, left: Standard Z-bend waveguide. Top, right: The optimized design. Bottom, left: TE polarized light propagating through the topology optimized Z-bend. Bottom, right: The manufactured device.

The idea of loss-less transmission of optical waves through photonic crystals outlined above is a truth with modifications. In reality, the transmission is less than 100% because of leaking waves and reflections at channel corners. It is quite obvious that the efficiency may be optimized by changing the shape, number and position of the holes along the channels. Therefore, the design of photonic crystals is an obviously interesting application for the topology optimization method.

Fig. 8 shows the result of the design process for a Z-bend. If we had just removed air holes to obtain a Z-shaped bend, the light transmitted through the bend would have been less than 50% due to losses and reflections. For topology optimization it was chosen to utilize only the outer parts of the two bend regions as design areas. Although one could choose much larger design areas, the numerical experiments showed that relatively small design areas were enough to yield the wanted improvement in efficiency. Had the efficiency been

unsatisfactory, the design areas could have been enlarged in order to introduce more freedom in the design. In order to reduce the bend loss, the transmitted energy flow measured by the Poynting vector through the Z-bend waveguide is maximized in the topology optimization procedure (see Fig. 8). The optimization can be performed for any number of frequencies simultaneously, e.g., in a min-max formulation. In the case of the Z-bend it was found that the use of a single frequency in the optimization is sufficient to produce a large bandwidth with low loss.

The result of the topology optimization process resulted in a close to 100% transmission in a wide frequency range. Fig. 8 shows the optimized design and the resulting wave propagation through the optimized waveguide. The optimized Z-bend was manufactured by e-beam lithography techniques at the Center for Optical Communication (COM) at DTU (see Fig. 8). The manufactured device performs very well with record breaking bandwidth and transmission properties.

4.2. Flow problems – initial steps

In fluid flow problems we are also faced with the problem of describing fields and material properties across interfaces, here between solid and fluid. In Borrvall and Petersson (2003) a model is suggested which in strong form is written as

$$\begin{aligned} \mu\,\nabla\cdot\left(\nabla\mathbf{u}+(\nabla\mathbf{u})^T\right)+\alpha\,\mathbf{u} &= \nabla p-\mathbf{f}\\ \nabla\cdot\mathbf{u} &= 0 \end{aligned} \tag{15}$$

where $\mathbf{u}$ is the velocity, p the pressure, $\mathbf{f}$ body forces and μ the dynamic viscosity of the fluid (for this and the subsequent PDEs we will assume that appropriate boundary conditions are given). The design coefficient α represents the porosity and we see that the extra term $\alpha\mathbf{u}$ (as compared to the Stokes flow problem) has the form of an absorption term, which ensures zero velocities at the penalized points controlled by α. Thus the variable α allows for fluid flow and (almost) solid to be covered in one model and one can formulate design problems that can determine the optimal lay-out of fluid flow.

Note that equation (15) is known as the Brinkman Equation (Gartling, Hickox and Givler, 1996) for the interpolation between Stokes flow and porous flow. In Borrvall and Petersson (2003) the model (15) is derived via a modelling of a Couette flow, i.e. a flow between plates with a distance of 2γ[2]. In that case we have $\alpha(\gamma)=\frac{5\mu}{2\gamma^2}$. However, with the interpretation as a Brinkman flow problem the idea generalizes to three dimensions also.

We are now ready to formulate the optimization problem. We will take $\gamma_e\in[\gamma_{\min},1]$ as the design variable and set $\alpha(\gamma)=\frac{5\mu}{2\gamma^2}$. A prescribed amount

[2]In order for this assumption to hold, it is assumed that the height of the channel is much smaller than the width.

of fluid is allowed in the design domain, i.e. the sum of the γ_e's is constrained. We want to minimize the energy dissipation in the system. This corresponds to maximizing the "flow compliance". The optimization problem may then in the FEM form be stated as

$$\begin{aligned} \min_{\boldsymbol{\gamma}} \quad & f = -\mathbf{F}^T\mathbf{U} \\ \text{s.t.} : \quad & \begin{bmatrix} \mathbf{K} & -\mathbf{G} \\ -\mathbf{G}^T & \mathbf{0} \end{bmatrix} \begin{Bmatrix} \mathbf{U} \\ \mathbf{P} \end{Bmatrix} = \begin{Bmatrix} \mathbf{F} \\ \mathbf{0} \end{Bmatrix} , \\ & \sum_{e=1}^{N} v_e\gamma_e \leq V^*, \quad 0 < \gamma_{\min} \leq \gamma_e \leq 1, \quad e = 1, \ldots, N \ . \end{aligned} \tag{16}$$

This optimization problem can be solved along similar lines as described earlier. We remark here that no penalization is required to obtain designs that only achieve the extreme values of the design parameter – the optimal design will automatically satisfy this objective (see Borrvall and Petersson, 2003, for the mathematical details).

4.2.1. Increasing the Reynolds number

Stokes flow is a linear problem with a Reynolds number $Re = 0$. Increasing Re results in a non-linear problem with increasing inertia forces. We simplify the problem by considering flows at moderate Reynolds numbers. Pipe flow can be assumed laminar up to approximately $Re = 2000$, thus as long as we stay well below this value, the flow field is stable and steady-state and the corresponding FE problem well-posed. The governing equations become

$$\begin{aligned} Re\ \mathbf{u}\cdot\nabla\mathbf{u} &= -\nabla p + \nabla\cdot\left(\nabla\mathbf{u} + (\nabla\mathbf{u})^T\right) + \mathbf{f} \\ \nabla\cdot\mathbf{u} &= 0 \end{aligned} \tag{17}$$

where all quantities are non-dimensional.

To gain control over the flow with optimization in mind, we use the absorption term introduced in the previous section. Further, we consider the case with no body forces $\mathbf{f} = \mathbf{0}$ and obtain

$$\begin{aligned} Re\ \mathbf{u}\cdot\nabla\mathbf{u} - \alpha(\gamma)\mathbf{u} &= -\nabla p + \nabla\cdot\left(\nabla\mathbf{u} + (\nabla\mathbf{u})^T\right) \\ \nabla\cdot\mathbf{u} &= 0 \ . \end{aligned} \tag{18}$$

The optimization problem for $Re > 0$ is therefore similar to (16) just with a non-linear FE problem representing the weak solution to (18). The sensitivity analysis should thus be modified to take this into account.

4.2.2. Examples

We show two examples of topology optimization in flow problems. The first is flow in a structure with two parallel inlets and outlets (Fig. 9); this example is repeated from Borrvall and Petersson (2003) and compare favourably to an example that can be found in Pironneau (1973). The second example illustrates the effect of inertia.

In Fig. 10 we demonstrate the difference between Stokes flow ($Re = 0$) and faster flow ($Re = 850$). We consider the design of a bend. The bend has sharp corners for Stokes flow, but the corners become rounder with increasing Reynolds number in response to the growth of the inertia term. Note however, that we had to relax the assumption behind the parabolic flow profile modelling in order to obtain this result. In order for the model to hold, the height of the channel should be small compared to the width. With this constraint, however, we find that inertia hardly has an effect on the optimal topology, hence the layout of micro fluidic channels is governed by the rule that the overall wall-length should be minimal. An implication of this is that the optimal 90 degree bend has sharp corners.

For other channel geometries (e.g. comparable width to height ratios), it is necessary to do a full 3D modelling and the conclusions above might be different.

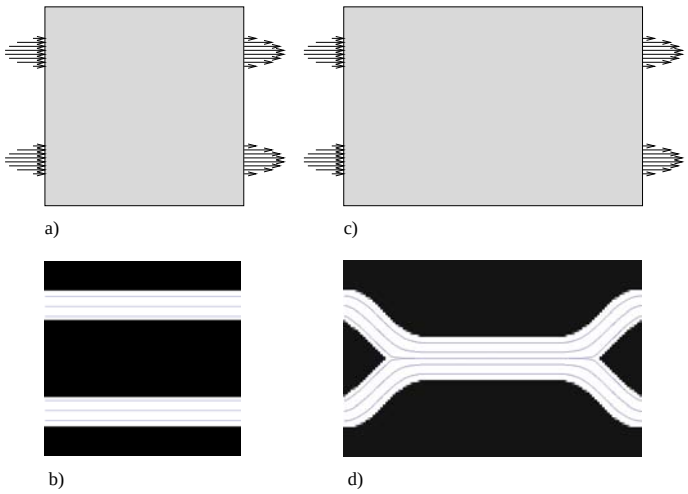

Figure 9. Minimization of flow resistance in structures with two parallel inlets and outlets for 30% fluid volume. a) Design domain with aspect ratio 1:1 and solution b). c) Design domain with aspect ratio 3:2 and solution d). The flow resistance of d) is 22% lower than for a topology with two straight pipes as in b) due to the lower resistance of the single wide channel.

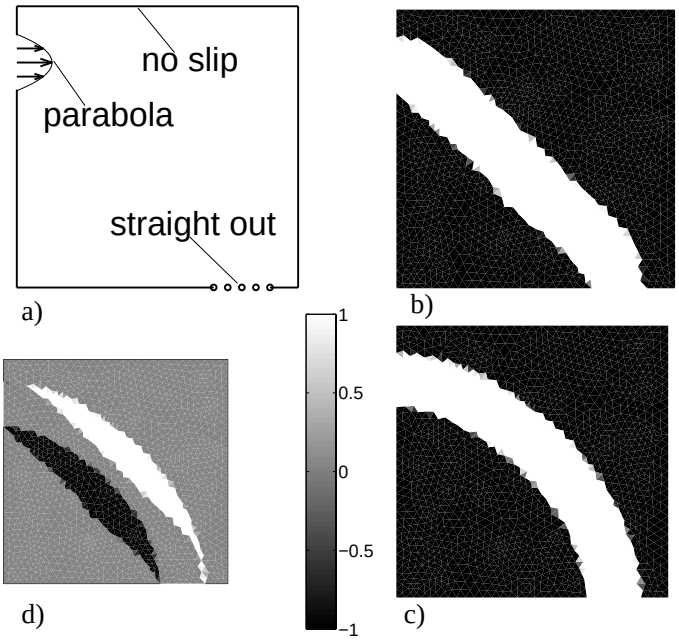

Figure 10. Design of a flow bend. a) Design domain and boundary conditions, b) topology optimized for $Re = 0$ c) topology optimized for $Re = 850$ and d) difference between c) and b).

For more discussion and examples of topology optimization on fluid flow problems with moderate Reynolds numbers we refer the reader to Gersborg-Hansen, Sigmund and Haber (2004). An important observation is that a large Reynolds number (larger than those associated with microfluidic devices) is required for inertia to have a significant effect on the design.

5. Other developments

The developments illustrated above represents only some of the work carried out in Denmark over the last years in connection with shape and topology design. This effort has not only been concerned with extending the basic notion to a broader range of structural design problems and to other engineering disciplines, but has also been concerned with the investigation of new concepts for modelling and of methods for improving computational performance (stability and speed).

5.1. Topology design

One of the important issues in topology design is the ability to control geometric features in the final design. This may be for production purposes as well as for more mundane reasons of controlling unwanted features of the computational results (such as artificial hinges in mechanism design). Recent work[3] on geometry control by applying a single and global constraint has been presented in Poulsen (2002a, 2003), while the application of concepts from multiscale analysis and wavelet design representations can be found in Poulsen (2002b), Yoon, Kim, Bendsøe and Sigmund (2004), and Chellappa, Diaz and Bendsøe (2004).

In the area of mechanics a method for design of support conditions for structures and mechanisms has been developed (Buhl, 2002). In the realm of mechanism design for snap behaviour for compliant mechanisms (Bruns, Sigmund and Tortorelli, 2002) and design of articulated mechanism has also been considered (Kawamoto, Bendsøe and Sigmund, 2004; Stolpe and Kawamoto, 2005). Here the latter work represents a new development in terms of the application of global optimization techniques. Also, much effort has been devoted to the development of concepts and analysis models for design for crashworthiness (see Pedersen, 2003a, 2004 and references therein), and developments of techniques for handling vibration problems can be found in Pedersen and Pedersen (2003) and Jensen and Pedersen (2005).

Related to the material design of band-gap materials mentioned earlier is the work on improving the buckling behaviour of composites (Neves, Sigmund and Bendsøe, 2002); other recent material design work can be found in Rodrigues, Guedes and Bendsøe (2002), Guedes, Rodrigues and Bendsøe (2003), and Pedersen (2003b).

Finally, as an illustration of the range of possibilities to apply the basic notion and computational techniques of topology design we mention the work by Bywater et al. (2004) on the design of proteins (molecular structures).

5.2. Shape design

In many situations the results of topology design requires refinement through the application of shape design. Moreover, many physical situations require *very precise* information about the interface between different media and in such cases the methods of shape design are crucial for succes. Here the strong position of Danish pump and wind-turbine industry has made it natural for a continued interest in this field, both for fluid-solid interaction problems (Lund, Møller and Jakobsen, 2002; Lund, Møller and Jakobsen, 2003) and for noise reduction problems (Langthjem and Olhoff, 2004a,b). In both cases the analysis and especially the sensitivity analysis poses great challenges in order to give reliable results for these very sensitive, nonlinear problems.

[3]In this and the following paragraphs we limit ourselves to references from 2002 and later.

In the realm of development of new approaches in this area work has also been performed on mixing ideas from shape design and topology design. Thus work on a geometry projection method (Norato et al., 2004) for shape design may also have implications for a level-set approach for topology design based on sensitivity analysis and mathematical programming.

6. Perspectives

In the sections above we have illustrated some of the possibilities for using the basic material density concept for topology design on a range of new problems, not only in structures, but also in other engineering areas.

One of the most interesting problem areas for future research will be the development of methods that can handle topology design of multiphysics problems where interfaces between phases have a central importance and where natural extensions of fields do not seem reasonable. The approach of extending fields over interfaces are central for the traditional material distribution method and has been succesfully applied in design of electrothermomechanical actuators (Jonsmann, Sigmund, Bouwstra, 1999).

Acknowledgements

The implementation of the method of moving asymptotes used in the work reported here was provided by Prof. Krister Svanberg from the Department of Mathematics at KTH in Stockholm. We thank Prof. Svanberg for allowing us to use his program. This work was supported, in part, by the the Danish Technical Science Research Council. This support is gratefully acknowledged.

References

Allaire, G., Jouve, F. and Toader, A.-M. (2004) Structural optimization using sensitivity analysis and a level-set method. *Journal of Computational Physics* **194** (1), 363–393.

Bendsøe, M.P. and Sigmund, O. (2003) *Topology Optimization - Theory, Methods and Applications*. Springer Verlag, Berlin Heidelberg.

Borel, P., Harpøth, A., Frandsen, L.H., Kristensen, M., Shi, J.S.J.P. and Sigmund, O. (2004) Topology optimization and fabrication of photonic crystal structures. *Optics Express* **12** (9), 1996–2001.

Borrvall, T. and Petersson, J. (2003) Topology optimization of fluids in Stokes flow. *International Journal for Numerical Methods in Fluids* **41**, 77–107.

Bourdin, B. and Chambolle, A. (2003) Design-dependent loads in topology optimization. *ESAIM: Control, Optimisation and Calculus of Variations* **9**, 19–48.

Bruns, T.E., Sigmund, O. and Tortorelli, D.A. (2002) Numerical methods for the topology optimization of structures that exhibit snap-through. *International Journal for Numerical Methods in Engineering* **55**, 1215–1237.

Buhl, T. (2002) Simultaneous topology optimization of structure and supports. *Structural and Multidisciplinary Optimization* **23** (5), 336–346.

Bywater, R., Poulsen, T.A., Røgen, P. and Hjorth, P.G. (2004) De novo generation of molecular structures using optimization to select graphs on a given lattice. *Journal of Chemical Information Theory and Computer Science* **44** (3), 856–86.

Chellappa, S., Diaz, A.R. and Bendsøe, M.P. (2004) Layout optimization of structures with finite-sized features using multiresolution analysis. *Structural and Multidisciplinary Optimization* **26** (1), 77–91.

Chen, B.-C. and Kikuchi, N. (2001) Topology optimization with design-dependent loads. *Finite Element in Analysis and Design* **37**, 57–70.

Du, J. and Olhoff, N. (2004a) Topological optimization of continuum structures with design-dependent surface loading - Part I: new computational approach for 2D problems. *Structural and Multidisciplinary Optimization* **27** (3), 151–165.

Du, J. and Olhoff, N. (2004b) Topological optimization of continuum structures with design-dependent surface loading - Part II: algorithm and examples for 3D problems. *Structural and Multidisciplinary Optimization* **27** (3), 166–177.

Eschenauer, H.A. and Olhoff, N. (2001) Topology optimization of continuum structures: A review. *Appl. Mech. Rev.* **54** (4), 331–390.

Foldager, J., Hansen, J.S. and Olhoff, N. (1998) A general approach forcing convexity of ply angle optimization in composite laminates. *Structural Optimization* **16** (2), 201–211.

Foldager, J.P., Hansen, J.S. and Olhoff, N. (2001) Optimization of the buckling load for composite structures taking thermal effects into account. *Structural and Multidisciplinary Optimization* **21** (1), 14–31.

Fuchs, M.B. and Moses, E. (2000) Optimal structural topologies with transmissible loads. *Structural and Multidisciplinary Optimization* **19**, 263–273.

Gartling, D., Hickox, C. and Givler, R. (1996) Simulation of coupled viscous and porous flow problems. *Compu. Fluid. Dyn.* **7**, 23–48.

Gersborg-Hansen, A., Sigmund, O. and Haber, R.B. (2004) Topology optimization of channel flow problems. *Structural and Multidisciplinary Optimization*, to appear.

Gibiansky, L.V. and Sigmund, O. (2000) Multiphase elastic composites with extremal bulk modulus. *Journal of the Mechanics and Physics of Solids* **48** (3), 461–498.

Guedes, J.M., Rodrigues, H.C. and Bendsøe, M.P. (2003) A material optimization model to approximate energy bounds for cellular materials under multiload conditions. *Structural and Multidisciplinary Optimization*,

25, 446-452.

Hammer, V. B., Bendsøe, M.P., Lipton, R. and Pedersen, P. (1997) Parametrization in laminate design for optimal compliance. *International Journal of Solids and Structures* **34** (4), 415–434.

Hammer, V.B. and Olhoff, N. (1999) Topology optimization with design dependent loads. In: C.L. Bloebaum, ed., *Proc. WCSMO-3, Third World Congress of Structural and Multidisciplinary Optimization*, CD-Rom.

Hammer, V.B. and Olhoff, N. (2000) Topology optimization of continuum structures subjected to pressure loading. *Structural and Multidisciplinary Optimization* **19**, 85–92.

Hammer, V.B. and Olhoff, N. (2001) Topology optimization of 3D structures with design dependent loads. In: G.D. Cheng, Y. Gu, S. Liu and Y. Wang, eds., *Proc. Second World Congress of Structural and Multidisciplinary Optimization*, Liaoning Electronic Press, Dalian, CD-rom.

Jensen, J.S. (2003) Phononic band gaps and vibrations in one- and two-dimensional mass-spring structures. *Journal of Sound and Vibration* **266** (5), 1053–1078.

Jensen, J.S. and Pedersen, N.L. (2005) On separation of eigenfrequencies in two-material structures using topology optimization: The 1D and 2D scalar cases. *J. Sound and Vibration*, to appear.

Jensen, J.S. and Sigmund, O. (2004) Systematic design of photonic crystal structures using topology optimization: Low-loss waveguide bends. *Applied Physics Letters* **84** (12), 2022–2024.

Jensen, J.S. and Sigmund, O. (2005) Topology optimization of photonic crystal structures using active sets: Design of a T-juntion waveguide. *J. Opt. Soc. Am. B*, to appear.

Jonsmann, J., Sigmund, O. and Bouwstra, S. (1999) Multi degrees of freedom electro-thermal microactuators. In: 'TRANSDUCERS'99', 1372–1375.

Kawamoto, A., Bendsøe, M.P. and Sigmund, O. (2004) Articulated mechanism design with a degree of freedom constraint. *International Journal for Numerical Methods in Engineering* **61** (9), 1520–1545.

Landau, L.D. and Lifshitz, E.M. (1975) *The Classical Theory of Fields, 4th ed.* Pergamon Press, Oxford.

Langthjem, M. and Olhoff, N. (2004a) A numerical study of flow-induced noise in a two-dimensional centrifugal pump. Part I. Hydrodynamics. *Journal of Fluids and Structures* **19** (3), 349–368.

Langthjem, M. and Olhoff, N. (2004b) A numerical study of flow-induced noise in a two-dimensional centrifugal pump. Part II. Hydroacoustics. *Journal of Fluids and Structures* **19** (3), 369–386.

Lund, E., Møller, H. and Jakobsen, L. (2003) Shape design optimization of stationary fluid-structure interaction problems with large displacements and turbulence. *Structural and Multidisciplinary Optimization* **25** (5-6), 383–392.

LUND, E., MØLLER, H. and JAKOBSEN, L.A. (2002) Shape optimization of fluid-structure interaction problems using two-equation turbulence models. In: *Proc. 43rd AIAA/ASME/ASCE/AHS/ASC Structures, Structural Dynamics, and Materials Conference and Exhibit*, 22 - 25 April 2002, Denver, Colorado, AIAA, CD-ROM.

LUND, E. and STEGMANN, J. (2005) On structural optimization of composite shell structures using a discrete constitutive parameterization. *Wind Enrgy* **8** (1), 109–124.

NEVES, M.M., SIGMUND, O. and BENDSØE, M.P. (2002) Topology optimization of periodic microstructures with a penalization of highly localized buckling modes. *International Journal for Numerical Methods on Engineering* **54** (6), 809–834.

NORATO, J., HABER, R., TORTORELLI, D. and BENDSØE, M.P. (2004) A geometry projection method for shape optimization. *International Journal for Numerical Methods in Engineering* **60** (14), 2289–2312.

OLHOFF, N. and DU, J. (2004) Topology optimization of vibrating structures with hydrodynamic surface pressure loading. In: *Proc. 21st International Congress of Theoretical and Applied Mechanics*, Warsaw, Poland, August 15-21, 2004, Institute of Fundamental Technological Research, Warsaw, Poland, CD-Rom.

PEDERSEN, C.B.W. (2003) Topology optimization for crashworthiness of frame structures. *International Journal of Crashworthiness* **8** (1), 29–40.

PEDERSEN, C.B.W. (2004) Crashworthiness design of transient frame structures using topology optimization. *Computer Methods in Applied Mechanics and Engineering* **193** (6-8), 653–678.

PEDERSEN, N. L. and PEDERSEN, P. (2003) Shape, position and orientational design of holes for plates with optimized eigenfrequencies. *Materials Science Forum* **440-441**, 321–328.

PEDERSEN, P. (2003) A note on design of fiber-nets for maximum stiffness. *Journal of Elasticity* **73** (3), 127–145.

PIRONNEAU, O. (1973) On optimal profiles in Stokes flow. *Journal of Fluid Mechanics* **59**, 117–128.

POULSEN, T.A. (2002a) A simple scheme to prevent checkerboard patterns and one-node connected hinges in topology optimization. *Structural and Multidisciplinary Optimization* **24** (5), 396–399.

POULSEN, T.A. (2002b) Topology optimization in wavelet space. *International Journal for Numerical Methods in Engineering* **53**, 567–582.

POULSEN, T.A. (2003) A new scheme for imposing a minimum length scale in topology optimization. *International Journal for Numerical Methods in Engineering* **57** (6), 741–760.

RODRIGUES, H.C., GUEDES, J.M. and BENDSØE, M.P. (2002) Hierarchical optimization of material and structure. *Structural and Multidisciplinary Optimization* **24** (1), 1–10.

Sigmund, O. (2001) A 99 line topology optimization code written in MATLAB. *Structural and Multidisciplinary Optimization* **21**, 120–127.

Sigmund, O. and Jensen, J.S. (2003) Systematic design of phononic band gap materials and structures by topology optimization. *Philosophical Transactions of the Royal Society A: Mathematical, Physical and Engineering Sciences* **361**, 1001–1019.

Sigmund, O. and Jensen, J.S. (2005) Systematic design of acoustic devices using topology optimization. Under preparation.

Sigmund, O. and Petersson, J. (1998) Numerical instabilities in topology optimization: A survey on procedures dealing with checkerboards, mesh-dependencies and local minima. *Structural Optimization* **16** (1), 68–75.

Sigmund, O. and Torquato, S. (1997) Design of materials with extreme thermal expansion using a three-phase topology optimization method. *Journal of the Mechanics and Physics of Solids* **45** (6), 1037–1067.

Stegmann, J. and Lund, E. (2005) Discrete material optimization of general composite shell structures. *International Journal for Numerical Methods in Engineering* **62** (14), 2009–2027.

Stolpe, M. and Kawamoto, A. (2005) Design of planar articulated mechanisms using branch and bound. *Mathematical Programming B*, published on-line, April 2005.

Svanberg, K. (1987) The method of moving asymptotes - A new method for structural optimization. *International Journal for Numerical Methods in Engineering* **24**, 359–373.

Svanberg, K. (2002) A class of globally convergent optimization methods based on conservative convex separable approximation. *SIAM Journal on Optimization* **12** (2), 555–557.

Wang, X., Wang, M.Y. and Guo, D. (2004) Structural shape and topology optimization in a level-set-based framework of region representation. *Structural and Multidisciplinary Optimization* **27** (1-2), 1–19.

Yoon, G.H., Kim, Y.Y., Bendsøe, M.P. and Sigmund, O. (2004) Hinge-free topology optimization with embedded translation-invariant differentiable wavelet shrinkage. *Structural and Multidisciplinary Optimization* **27** (3), 139–150.